

**Tellurorhodamine photocatalyzed aerobic oxidation of
organo-silanes and phosphines by visible-light**

Journal:	<i>Dalton Transactions</i>
Manuscript ID	DT-ART-02-2019-000487.R2
Article Type:	Paper
Date Submitted by the Author:	28-Mar-2019
Complete List of Authors:	Rettig, Irving; Portland State University, Chemistry Van, Jackson; Portland State University, Chemistry Brauer, Jacob; Portland State University, Chemistry Luo, Wentai; Portland State University, Chemistry McCormick, T.; Portland State University, Chemistry

Tellurorhodamine photocatalyzed aerobic oxidation of organo-silanes and phosphines by visible-light

Irving D. Rettig, Jackson Van, Jacob B. Brauer, Wentai Luo, Theresa M. McCormick*

Department of Chemistry, Portland State University, Portland, Oregon, 97201, USA

*t.m.mccormick@pdx.edu

Abstract

Tellurorhodamine, 9-mesityl-3,6-bis(dimethylamino)telluroxanthylum hexafluorophosphate (**1**), photocatalytically oxidizes aromatic and aliphatic silanes and triphenyl phosphine under mild aerobic conditions. Under irradiation with visible light, **1** can react with self-sensitized $^1\text{O}_2$ to generate the active telluroxide oxidant (**2**). Silanes are oxidized to silanols and triphenyl phosphine is oxidized to triphenyl phosphine oxide either using **2**, or **1** with aerobic irradiation. Kinetic experiments coupled with a computational study elucidate possible mechanisms of oxidation for both silane and phosphine substrates. First-order rates were observed in the oxidation of triphenyl phosphine and methyl-diphenyl silane, indicating a substitution like mechanism for substrate binding to the oxidized tellurium(IV). Additionally, these reactions exhibited a rate-dependence on water. Oxidations were typically run in 50:50 water/methanol, however, the absence of water decreased the rates of silane oxidation to a greater degree than triphenyl phosphine oxidation. Parallel results were observed in solvent kinetic isotope experiments using D_2O in the solvent mixture. The rates of oxidation were slowed to a greater degree in silane oxidation by **2** ($k_{\text{H}}/k_{\text{D}} = 17.30$) than for phosphine ($k_{\text{H}}/k_{\text{D}} = 6.20$). Various silanes and triphenyl phosphine were photocatalytically oxidized with **1** (5%) under irradiation with warm white LEDs using atmospheric oxygen as the terminal oxidant.

1 Introduction

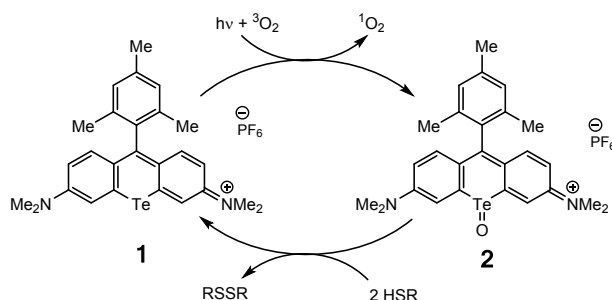
Over the past decade, there has been a tremendous push to develop catalysts for green synthetic methods within the field of organic chemistry.^{1,2} Catalysts that have been employed in oxidation reactions represent one such avenue of research, however, the utility of many catalytic oxidation reactions is limited due to the generation of stoichiometric amounts of co-oxidant waste.³ Using molecular oxygen as the stoichiometric oxidant in catalytic oxidation reactions avoids this issue due to its high relative abundance, low cost and negligible environmental toxicity.

One method of utilizing molecular oxygen in aerobic catalytic oxidation reactions is through the generation of photosensitized singlet oxygen ($^1\text{O}_2$) from ground state triplet oxygen ($^3\text{O}_2$). Typically, inorganic metal-containing chromophores with strong spin-orbit coupling are used to photosensitize $^1\text{O}_2$.⁴ The most common of these complexes involve a heavy metal center, like iridium, ruthenium or osmium, with bipyridine-type ligands.^{5,6} Though extensive research in ligand modifications on these chromophores have allowed for improved $^1\text{O}_2$ generation, the oxidation reactions are equally limited by the low selectivity of transient $^1\text{O}_2$ and its radical-type chemistry.⁷⁻¹⁰ Organic photosensitizers like Rose Bengal, Erythrosin blue, and Methylene blue have been developed to directly address the economic and environmental setbacks of metal-containing photosensitizers, however, these dyes are reactive towards $^1\text{O}_2$, and, in many cases, have decreased stability in solution because of $^1\text{O}_2$ induced degradation.¹¹

These major challenges in aerobic oxidation photocatalysis can be addressed by using the photosensitized $^1\text{O}_2$ to generate longer-lived reactive intermediates that will selectively oxidize desired substrates. In an effort to address this, Ando and coworkers developed a series of biaryl organotellurium compounds that could react with $^1\text{O}_2$ generated

by an external organic photosensitizer to form a considerably more selective oxidant than $^1\text{O}_2$ alone.¹² $^1\text{O}_2$ oxidizes the Te(II) compound to Te(IV), which can then reduce upon interaction with a substrate to regenerate the initial Te(II) compound. Using this method, Ando reported successful photocatalytic aerobic oxidation of phosphite esters, silanes and thiols.^{13–15} However, in each case, an external photosensitizer was needed to initially generate $^1\text{O}_2$. Detty and coworkers have developed tellurium-based organic dyes that react with $^1\text{O}_2$, in a similar vein to the diaryl telluride compounds but also generate the required $^1\text{O}_2$.^{16–18}

We have previously published that a tellurium-based rhodamine analog **1** can form telluroxide **2** upon irradiation with visible light, and then reduce back to **1** by oxidizing various thiols to their corresponding disulfides, shown in Scheme 1.¹⁹



Scheme 1. Oxidation of **1** to **2** with light and $^3\text{O}_2$, generating $^1\text{O}_2$ which directly oxidizes **1**. Two equivalents of thiol can be reductively eliminated from **2** to return **1**.

This net oxidative transformation was characterized as having a substitution-like mechanism via a dithio-tellurane intermediate. A transfer of the oxygen atom to the substrate was not involved in the thiol oxidation mechanism.

Phosphine and silane oxidation are two industrially relevant chemical reactions that involve oxygen atom transfer that can be accessed via aerobic oxidation catalysis. In particular for silane oxidation, noble metal catalysts and nano-materials are typically used for reactions of this type.^{20–23} Oxidized diaryl tellurium-containing compounds have been observed to reduce in the presence of both silanes and phosphite esters,^{13,15} However,

experimentally supported mechanisms for the oxygen transfer by telluroxides have yet to be explored. Additionally, oxidation of phosphines and silanes by **2** has not been reported, in which the only reactants required to oxidize these substrates is light, oxygen and water. We propose two different mechanisms involving oxygen transfer from **2** to afford the experimentally observed phosphine oxides and silanols, supported by kinetic experiments and computations.

2 Experimental

All reagents and solvents were purchased from Sigma Aldrich and Tokyo Chemical Industry (TCI). Experiments requiring anhydrous conditions were performed using Schlenk line techniques or in a nitrogen-containing glovebox. The synthesis of **1** is detailed in the Supporting Information. $^1\text{H}/^{13}\text{C}$ NMR spectra (Figure S1-2) and Uv-Vis absorption spectra (Figure S3) of **1** are consistent with previously published literature values.²⁴

Oxidation of phosphines or silanes using 2

A bulk solution of **2** was prepared to allow us to study the oxidation of different substrates by **2**, which is the proposed catalyst turnover step. Photo-oxidation of **1** to **2** was performed using previously published methods¹⁹ A solution of **1** in aqueous methanol (50 mmol, 5.4×10^{-4} M) was irradiated with warm white light LEDs while stirring for approximately 8 hours. The absorbance maxima of **1** and **2**, (600 nm and 665 nm respectively) in methanol were used to monitor the formation of **2** in situ.²⁴ After the UV-Vis spectra of **2** persisted (no further oxidation), the solution was evaporated to dryness and stored in the dark as a teal residue for use in preparing solution for both UV-Vis absorption and $^1\text{H}/^{13}\text{C}$ NMR spectroscopic experiments.

UV-Vis Spectroscopy

UV-Vis absorption spectroscopy was used to elucidate kinetic and mechanistic details for the reduction of **2** to **1** by phosphines and silanes. Rates for oxidation of triphenyl phosphine and various silanes were determined using pseudo-first order reaction conditions. In each experiment, a solution of **2**, ranging from 2.4×10^{-6} M to 5.4×10^{-6} M, was prepared in 50:50 methanol/water (unless specified otherwise) and spiked with excess (20-100 equivalents, experiment specific) of reductant and sealed. Spectra were acquired between 400-800 nm every 30 seconds for 5 to 15 min and were baseline corrected in each case. Reactions that took longer than 15 minutes to complete were stirred continuously between scans, which were then acquired every 5 minutes. Reaction rates were calculated from the natural log of the concentration of **2** over time. The concentration of **2** was determined by the Beer's law equation using the absorbance at 665 nm and molar extinction coefficient for **2** used was $9.5 \times 10^4 \text{ M}^{-1} \text{ cm}^{-1}$, as reported by Detty *et. al.*²⁴

¹H/¹³C NMR

¹H/¹³C NMR experiments were conducted using a 600 MHz Bruker NMR spectrometer. Phosphines and silanes were oxidized catalytically using 5 mol % of **1** in methanol-d₄. Samples were prepared under oxygen atmosphere with **1** (1.0×10^{-3} M), 20 eq of reductant (phosphine or silane) (3.0×10^{-2} M), 5% water, and cyclohexane as an internal standard in a 5 mm Wilmad Lab-Glass low-pressure/vacuum NMR tube. To ensure sufficient gas exchange, the tubes were stirred via inversion using a custom-made rotating stage mounted inside of a white-light LED chamber.

Mass Spectrometry

Mass spectrometry identified the oxidized products of photocatalytic oxidation of both silanes and phosphines with **1**. Samples were prepared with **1** (1.0×10^{-3} M), 20 eq of reductant (phosphine or silane) (3.0×10^{-2} M) and 5% water in methanol with an oxygen atmosphere. Triphenyl phosphine and aromatic and aliphatic silanes were oxidized for the same period of time as in the NMR experiments (18-24 hours). Samples were diluted to 100 ng/ μ l before analysis. Agilent (Santa Clara, California, USA) 7693 autosampler, Agilent 7890A GC and Agilent 5975C MS was used for the analysis. The GC column was Restek (Bellefonte, PA) Rxi-5Sil MS of 30 m length, 0.25 mm id and 0.25 mm film thickness. One microlitre of the sample solution was injected on the GC injector at 225 °C with a 20:1 split. The GC temperature program for all analyses was: 80°C hold for 2 min; 15°C/min to 300°C; hold at 300°C for 1 min; then 15°C/min to 320°C. The MS operated in electron impact ionization mode. The MS source temperature was 225 °C and the scan range was 34 to 400 amu. The identifications were made by matching the mass spectra of characterized compounds to their NIST library mass spectra or the mass spectra generated from pure compounds purchased from Sigma Aldrich and the GC retention times of the compounds.

Computational Details

Calculations were completed with Gaussian09²⁵ suit of programs, and results were visualized using GaussView05.²⁶ The structures were optimized to a minima using the B3LYP^{27–29} level of theory with a split basis set (6-31+G(d))^{30–32} for all light atoms, LanL2DZ^{33–35} for Te). Gibbs free energies were obtained from thermally corrected energy values from the frequency calculations on minimized structures. Hirshfeld charge population analyses were calculated from optimized geometries.^{36,37}

3 Results and Discussion

Stoichiometric reduction of 2 to 1

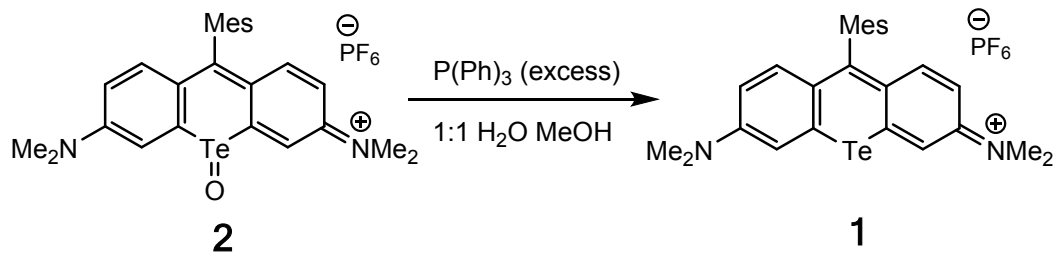
Information about the reduction step of the catalytic cycle was obtained from kinetic experiments on reduction of **2** to **1** with varying amounts of excess substrate. Compound **2** was prepared by irradiating a solution of **1** under atmospheric conditions and the solvent was removed. We monitored the reaction between **2** and both phosphines and silanes using UV-Vis spectroscopy to determine the concentration of **1** and **2** over time using previously published photophysical data (Table 1). The overall rates of both phosphine and silane oxidation are slow enough that standard UV-Vis spectroscopic methods can be used to monitor the reaction. This is $\sim 10^3$ times slower than our previously reported rates of oxidation of aromatic thiols by the reduction of **2** to **1**.¹⁹

Table 1. Photophysical information for **1** and **2**.²⁰

Compound	Absorbance maximum (nm)	Molar extinction coefficient ($M^{-1}cm^{-1}$)	Singlet oxygen quantum yield (ϕ)
1	600	86,000	0.75 \pm 0.03
2	665	95,000	n/a ^a

^aTriplet quantum yields are not available for **2** due to fluorescent emission.

To determine the rate constants for the oxidation reactions, the concentration of **2** was determined by monitoring the absorption at 665 nm over time, after the addition of various concentrations of the reductants. Scheme 2 shows the reaction conditions for stoichiometric oxidation of triphenyl phosphine oxidation by **2**.



Scheme 2. Stoichiometric reduction of **2** by excess triphenyl phosphine. Various concentrations of triphenyl phosphine were reacted with **2** (2.4×10^{-6} M) and monitored by UV-Vis spectroscopy.

Rates were determined for a range of concentrations of triphenyl phosphine (2.4×10^{-5} M, 4.8×10^{-5} M, 7.2×10^{-5} M, 9.6×10^{-5} M) with **2** (2.4×10^{-6} M) in 50:50 water/methanol. The UV-Vis traces of **2** reducing to **1** with 30 eq of triphenyl phosphine (7.2×10^{-5} M) are shown in Figure 1a. Full conversion of **2** to **1**, indicated by the disappearance of the peak at 665 nm and persistence of the peak at 600 nm, occurred within 15 minutes. An isosbestic point is observed at 618 nm indicating direct conversion from **2** to **1**. The natural log of the concentration of **2**, when plotted against time, gave a linear fit (Figure 1b). Plotting these rates against the concentrations of triphenyl phosphine gave a pseudo-first-order rate constant of $16.67 \text{ M}^{-1} \text{ s}^{-1}$ (Figure 1 insert). The observed linear relationship between the concentration of triphenyl phosphine and time would suggest a first order reaction.

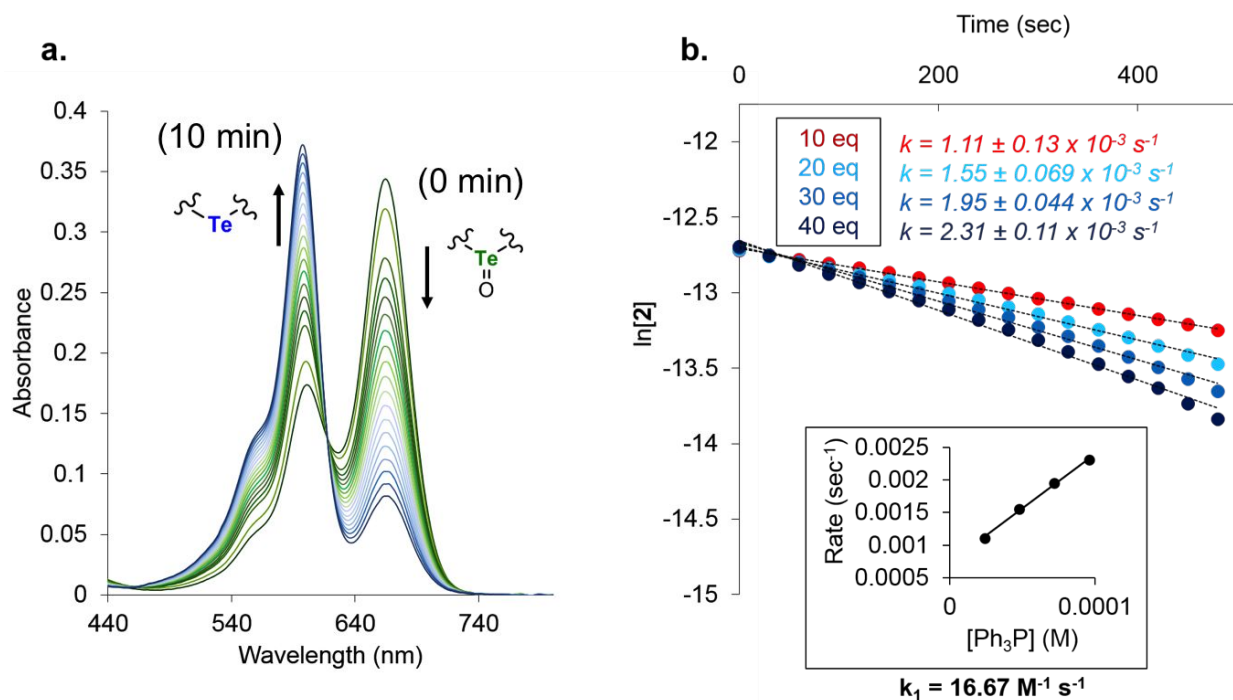
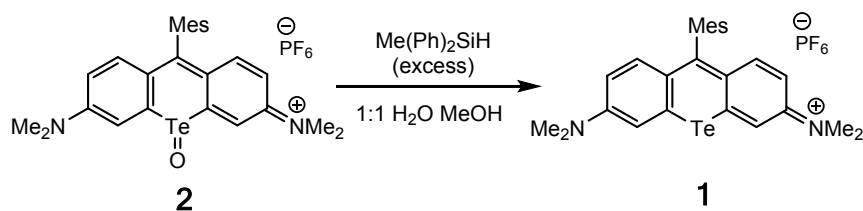


Figure 1. a) Example UV-Vis absorbance spectra of reduction of **2** to **1** with 30 eq triphenyl phosphine, b) natural log of the concentration of **2** versus time at increasing concentrations of triphenyl phosphine and the corresponding rate constant plot as the insert in 1b.

We determined the stoichiometry of this reaction by adding half or one stoichiometric equivalent of triphenyl phosphine to **2** ($5.4 \times 10^{-6} \text{ M}$) in methanol and stirred in the dark for two hours. The half equivalent sample had nearly equal amounts of **2** and **1** present. One equivalent of triphenyl phosphine was sufficient to fully reduced **2** to **1** (Figure S4). We later used this stoichiometry in conjunction with computational modeling to propose a reaction mechanism for oxygen transfer from **2** to phosphine to afford the corresponding phosphine oxide.

The kinetics of silane to silanol oxidation by **2** was also explored experimentally. Initially, triphenyl silane was selected as an appropriate analog to triphenyl phosphine to determine reaction kinetics, however, the reaction of **2** with 100 equivalents of triphenyl silane took 11 hours to fully reduce (Figure S5). Instead, diphenyl methyl silane was oxidized by **2**

within 5 min and was used to determine rates of silane oxidation. Scheme 3 shows the reaction conditions for stoichiometric methyl diphenyl silane oxidation by **2**.



Scheme 3. Stoichiometric reduction of **2** with excess methyl diphenyl silane. Various concentrations of silane were reacted with **2** (5.4×10^{-6} M) and monitored by UV-Vis spectroscopy.

Akin to phosphine oxidation experiments, various concentrations of diphenyl methyl silane (5.4×10^{-5} M, 1.1×10^{-4} M, 1.6×10^{-4} M, 2.2×10^{-4} M, 2.7×10^{-4} M) were reacted with **2** (5.4×10^{-6} M) to determine substrate dependence on reaction kinetics. Full reduction of **2** to **1** occurred between 5-15 minutes, dependent on silane concentration. Plots of the concentration of **2** versus time gave exponential decays (Figure 2a). Taking the natural log of the concentration of **2** gave linear traces (Figure 2b), corresponding to pseudo-first-order reaction rates. These were plotted against the concentration of methyl diphenyl silane to give a rate constant of $31.18 \text{ M}^{-1} \text{ s}^{-1}$ (Figure 2 insert). Attempts to stoichiometrically reduce **2** with one equivalent of silane resulted in only partial return of **1** due to the slow reaction kinetics at these low concentrations.

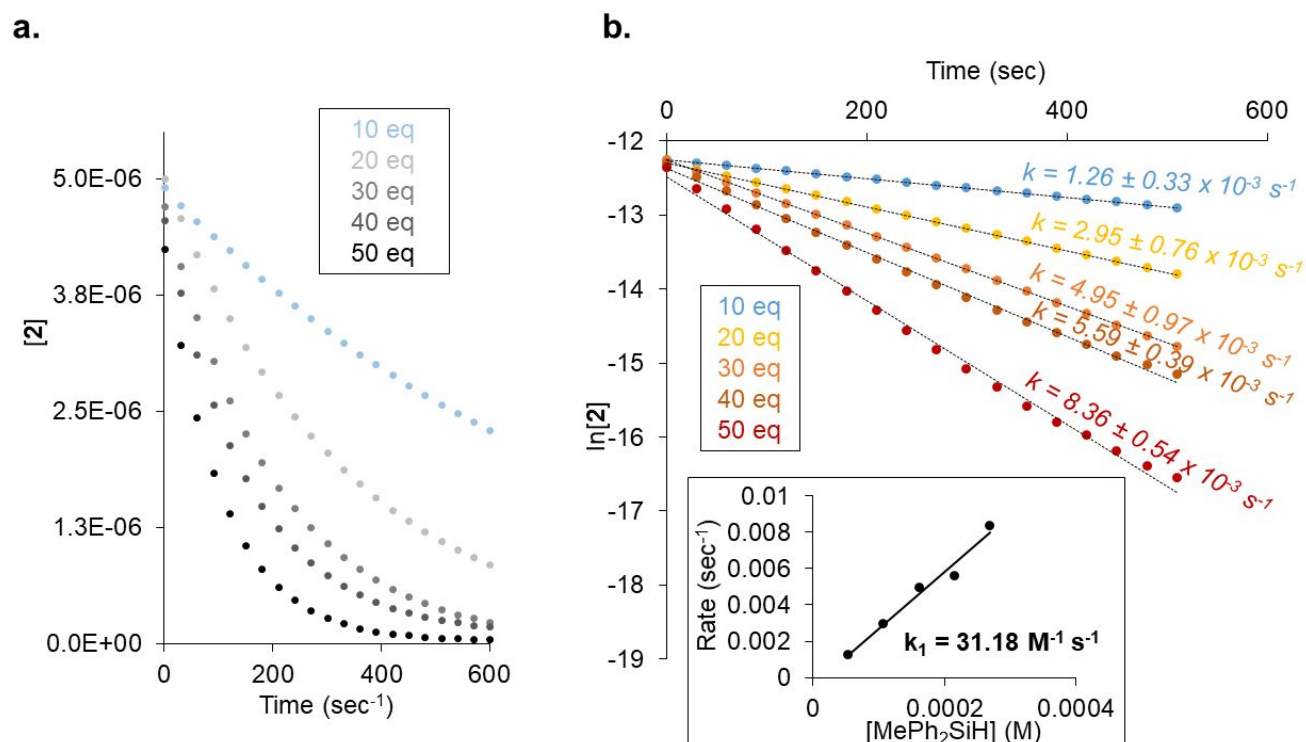


Figure 2. a) Pseudo-first-order rate plots of **[2]** at various concentrations of methyl diphenyl silane with respect to time, b) linear traces obtained by taking the natural log of **[2]** versus time and the corresponding rate constant plot in the insert.

Effect of water on reaction rates

We had previously determined that water plays a possible role in the substitution-like mechanism of thiol oxidation.¹⁹ The rates of phosphine and silane oxidation under anhydrous conditions were determined to elucidate the role of water in each reaction.

The ratio of the reaction rates under wet (k_{wet}) and dry (k_{dry}) conditions can be compared to determine the role of water in directly or indirectly solvating the reaction. The observed pseudo-first-order rates were slower under dry conditions in each case. Under anhydrous conditions, the pseudo-first order rate of triphenyl phosphine (2.2×10^{-5} M) reacting with **2** (5.4×10^{-6} M) was measured at $6.06 \pm 1.2 \times 10^{-4} \text{ s}^{-1}$ (k_{dry}). In the aqueous solvent mixture, the pseudo-first-order rate was $1.62 \pm 0.4 \times 10^{-3} \text{ s}^{-1}$ (k_{wet}), which when

compared gives a ratio of 2.67. Computational details show that the phosphine-bound intermediate **2-P**, as discussed below, has partial negative and positive charges located on the tellurium-bound oxygen and phosphine atoms respectively. In this case, because water is more polar than methanol, water solvation could stabilize intermediate **2-P**. This increased stabilization due to water solvation could explain the increase in reaction kinetics in aqueous versus neat methanol.

Under the same conditions, the rate of reaction between methyl diphenyl silane (2.2×10^{-5} M) and **2** (5.4×10^{-6} M) was $2.61 \pm 0.28 \times 10^{-5} \text{ s}^{-1}$, compared to $1.04 \pm 0.017 \times 10^{-3} \text{ s}^{-1}$ in the wet reaction. Dividing $k_{\text{wet}}/k_{\text{dry}}$ gives a ratio of 39.85, considerably higher than $k_{\text{wet}}/k_{\text{dry}}$ of triphenyl phosphine. The large difference in the rates between wet and dry conditions shows the significance of water solvation effects in silane oxidation by **2**. The computationally proposed intermediate **2-Si**, as discussed below, has both a hydroxyl group that can participate in hydrogen bonding and a partially negative silane group attached to the tellurium core that can be solvated by water. Stabilization from these multiple solvent interactions could account for the slowed kinetics in anhydrous solvent. Additionally, because $k_{\text{wet}}/k_{\text{dry}}$ of both oxidation reactions differ from one another, it can be said that water dependence varies with substrate and that the role of water is different in silane oxidation than in phosphine oxidation.

Solvent kinetic isotope effect

To further explore the role of water solvation in these reactions, substrate oxidation by **2** was carried out in deuterium oxide (D_2O) and methanol to measure the solvent kinetic isotope effect. When D_2O was substituted for H_2O , the reduction of **2** to **1** by triphenyl phosphine (2.2×10^{-5} M) under pseudo-first order conditions was much slower, with a rate of $2.61 \pm 0.5 \times 10^{-4} \text{ s}^{-1}$ versus $1.62 \pm 0.4 \times 10^{-3} \text{ s}^{-1}$ at the same concentration in 50:50 $\text{H}_2\text{O}/$

MeOH. The kinetic isotope effect in this case is 6.20, suggesting that water plays a direct role in solvating the reaction of phosphine oxidation by **2** via hydrogen bonding.^{34,35}

When reacting methyl diphenyl silane with **2** in 50:50 D₂O/ MeOH, the pseudo-first-order rate was observed to be $6.01 \pm 0.14 \times 10^{-5} \text{ s}^{-1}$. In H₂O/ MeOH this was $1.04 \pm 0.017 \times 10^{-3} \text{ s}^{-1}$. A kinetic isotope effect of 17.30 was obtained in this case, which is too large to be described by a single proton exchange. Compounding primary and secondary kinetic isotope effects can occur when more than one proton is involved in exchanging with and solvating a reaction intermediate.^{36,37} This large kinetic isotope effect could therefore be the result of proton exchange from solvent, like in the dehydration step to produce **2-Si** shown below, as well as hydrogen-bonding stabilization from other solvent molecules of this intermediate.

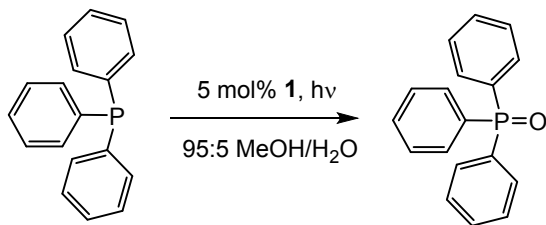
Catalytic substrate oxidation by 1

Phosphine and silanes were oxidized catalytically to their corresponding phosphine oxides and silanols with 5% **1**. ¹H/¹³C HNMR spectroscopy was used to monitor the conversion of starting materials to products (Figure S6-15). Yields were quantified using cyclohexane as an internal standard, comparing the integration ratio of standard to starting material and standard to products in each ¹H NMR spectrum. The scope of the reactants successfully oxidized to their corresponding phosphine oxide and silanol analogs are compiled in Table 2.

Table 2. Scope of photocatalytic phosphine and silane oxidation using 5% **1** in methanol-*d*₄ irradiated with warm white LEDs and monitored by ¹H NMR

entry	reactant	irradiation time (h)	product conversion (%)	Yield (%)
1	triphenyl silane	24	96	85
2	methyl diphenyl silane	18	99	98
3	dimethyl phenyl silane	18	≥99	99
4	triethyl silane	18	≥99	95
5	triphenyl phosphine	18	≥99	≥99

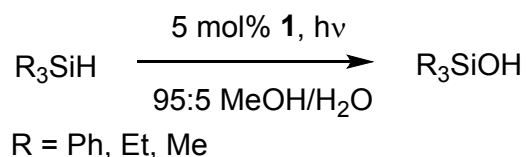
Triphenyl phosphine was catalytically oxidized to triphenyl phosphine oxide in methanol-*d*₄ within 18 hours by **1** with quantitative yield, shown in Scheme 4.



Scheme 4. Catalytic oxidation of triphenyl phosphine with 5 mol% of **1**. Reactions were run in an oxygen atmosphere and irradiated with light for 18 hours.

To determine if **1** was responsible for the catalytic oxidation of triphenyl phosphine or ¹O₂ directly, a ¹O₂ photosensitizer (Rose Bengal) (1.0 x 10⁻³ M) was combined with triphenyl phosphine (3.0 x 10⁻² M) and irradiated under the same reaction conditions and analyzed by GCMS. After 18 hours, a mass peak of 277 m/z was observed, which indicates the presence of triphenyl phosphine oxide (Figure S16). Although one would expect competing reaction between ¹O₂ and **2**, **2** gets formed very rapidly, as shown in our previously published work.¹⁹ The proximity of ¹O₂ to the tellurium core after formation could increase its likelihood of reacting with tellurium versus phosphine. Furthermore, we have shown that triphenyl phosphine can react with **2** in the dark to form triphenyl phosphine oxide and **1**. Thus, ¹O₂ or photocatalytically formed **2** could result in the observed phosphine oxidation.

Catalytic oxidation of both aromatic and aliphatic silanes to their corresponding silanols were obtained with 5% **1** in methanol-*d*4 within 18-24 hours of irradiation, shown in Scheme 5. Nearly all silanols were obtained in quantitative yields, as determined by ¹H NMR spectroscopy.



Scheme 5. General catalytic oxidation of silanes with 5 mol% of **1**. Reactions were run in an oxygen atmosphere and irradiated with light for 18-24 hours.

The disappearance of the silane proton peak was observed in all cases, as well as an up field shift in the alpha-carbon protons of the aliphatic and aromatic moieties. Unlike the other silanes, after 24 hours triphenyl silane had only partially oxidized, evidenced by the persistence of the silane proton peak in the ¹H NMR spectrum. As seen in the above rate studies, the large steric bulk of triphenyl silane significantly slows the reaction with **2**, which could account for increased time of oxidation and the less than quantitative yield. A control experiment was also conducted to determine if ¹O₂ could oxidize silane to silanol with Rose Bengal (Figure S17). Conditions and concentrations for the control were replicated with triethyl silane (1.0 x 10⁻³ M) and photosensitizer (3.0 x 10⁻² M) in 95:5 MeOD/H₂O. After 24 hours of irradiation, the ¹H NMR spectrum of silane was unchanged. This not only indicates that silane does not react with ¹O₂ generated *in situ* but that the silane is unreactive towards water under these conditions.

Catalytic phosphine and silanol formation were confirmed with GC-MS. Samples were prepared using the NMR experimental conditions, but with non-deuterated solvent. Triphenyl phosphine and aromatic and aliphatic silanes were oxidized for the same period of time as in the NMR experiments (18-24 hours). For triphenyl phosphine oxidation, a peak at 277 m/z

was the only peak observed in the spectrum, which corresponds to triphenyl phosphine oxide (Figure S18). Silane oxidation products were also characterized with GCMS. Masses of 276, 214, 152, and 132 m/z were obtained, matching the reference mass peaks of triphenyl silanol, methylphenyl silanol, dimethylphenyl silanol and triethyl silanol respectively (Figure S18-21). A large peak appeared in each sample 14 mass units above the molecular ion peak. This indicates solvent exchange wherein $-OMe$ interchanges with the $-OH$ of each silanol (Figure S22-25). Another common byproduct of silane oxidation is disiloxane caused by unfavorable condensation. A small mass peak in the triethyl silane oxidation sample correlated to the corresponding disiloxane (Figure S26). However disiloxane formation was not observed for any other tested silane even in aqueous conditions. We suggest the low steric bulk of the ethyl moieties significantly increases ease dimerization of the silanol product compared to the bulkier substrates.^{38,39}

Computationally supported mechanism

DFT methods were used to further elucidate potential mechanisms of phosphine and silane oxidation by **2**. Thermal and free energy corrected to total energy values of the optimized structures were used to calculate the Gibbs free energy changes (ΔG) between reactants and products. To reduce overall computational time, trimethyl phosphine and trimethyl silane were used to model the mechanisms of oxidation. Calculations included implicit water solvation to reflect experimental findings.

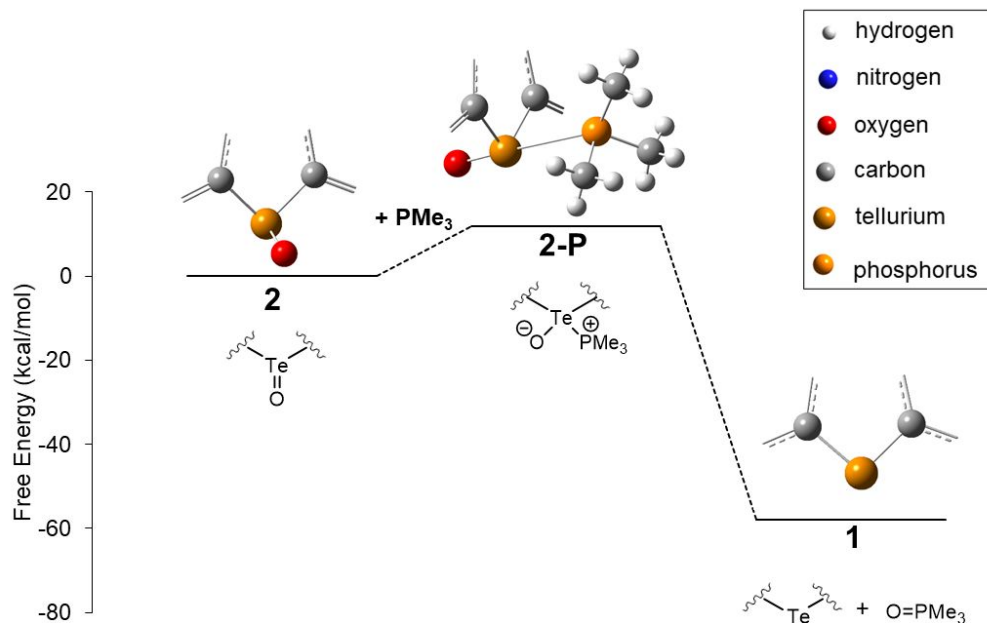


Figure 3. Reaction coordinate of trimethyl phosphine oxidation by **2**.

The reaction coordinate diagram of trimethyl phosphine oxidation by **2** is shown in Figure 3. The first step in the proposed reaction pathway is the binding of phosphine to the tellurium (IV) core of **2** to give **2-P**, which has a ΔG of 11.97 kcal/mol. Hirshfeld charge analysis was used to determine the change in electron density at the tellurium core between **2** and **2-P** to verify the bonding interaction. A decrease in positive charge density is observed at the tellurium atom, 0.39 in **2** and 0.34 in **2-P**, which indicates electron donation from the phosphorus atom to the tellurium. The Te-P bond length of 3.59 Å is within the sum of van der Waals radii for tellurium and phosphorus, further supporting bond formation in the **2-P** intermediate.

We have previously reported that **2** can react with water to form a hydrated intermediate **2a**, shown below.¹⁹ In this case, substitution of phosphine at the Te atom in **2a** to generate monophospho-hydroxy tellurane is energetically unfavorable, with a ΔG of +68.55

kcal/mol in vacuum. Including water solvation in the calculation of this intermediate resulted in a structural minimum where neither the phosphine nor hydroxyl group were still attached to the tellurium core. Direct substitution of **2**, in phosphine oxidation without proceeding through a hydrated intermediate first is a new mechanistic prediction based on experimental and computational results. Following the binding of phosphine to form **2-P**, reductive elimination of trimethyl phosphine oxide regenerated **1** with a ΔG of -69.80 kcal/mol. The overall ΔG_{rxn} of phosphine oxidation by **2** was calculated to be -57.83 kcal/mol. This mechanism supports stoichiometric experimental results that one equivalent of phosphine is sufficient reduce **2** to **1**.

We also propose a mechanism for silane oxidation, which reflects a different pathway to silanol formation. This mechanism more closely resembles the mechanism of thiol oxidation by **2** by proceeding through hydrated intermediate **2a**.¹⁹ The reaction coordinate diagram of silane oxidation is shown in Figure 4. The initial reaction step is the binding of water by **2** to form **2a** which has a ΔG of 9.44 kcal/mol. Following this is the substitution of one of the hydroxyl groups for one moiety of silane to generate **2-Si** and water, which results in the silane bound to the tellurium core in a seesaw conformation. Without the inclusion of a water solvation model, the calculated ΔG of silane substitution was 8.93 kcal/mol; however, including the water solvation model reduced this ΔG to 0.47 kcal/mol. Reductive elimination of silanol regenerates **1**, which has a ΔG of -70.88 kcal/mol. The overall ΔG_{rxn} for the oxidation of trimethyl silane to trimethyl silanol by **2** is -60.97 kcal/mol.

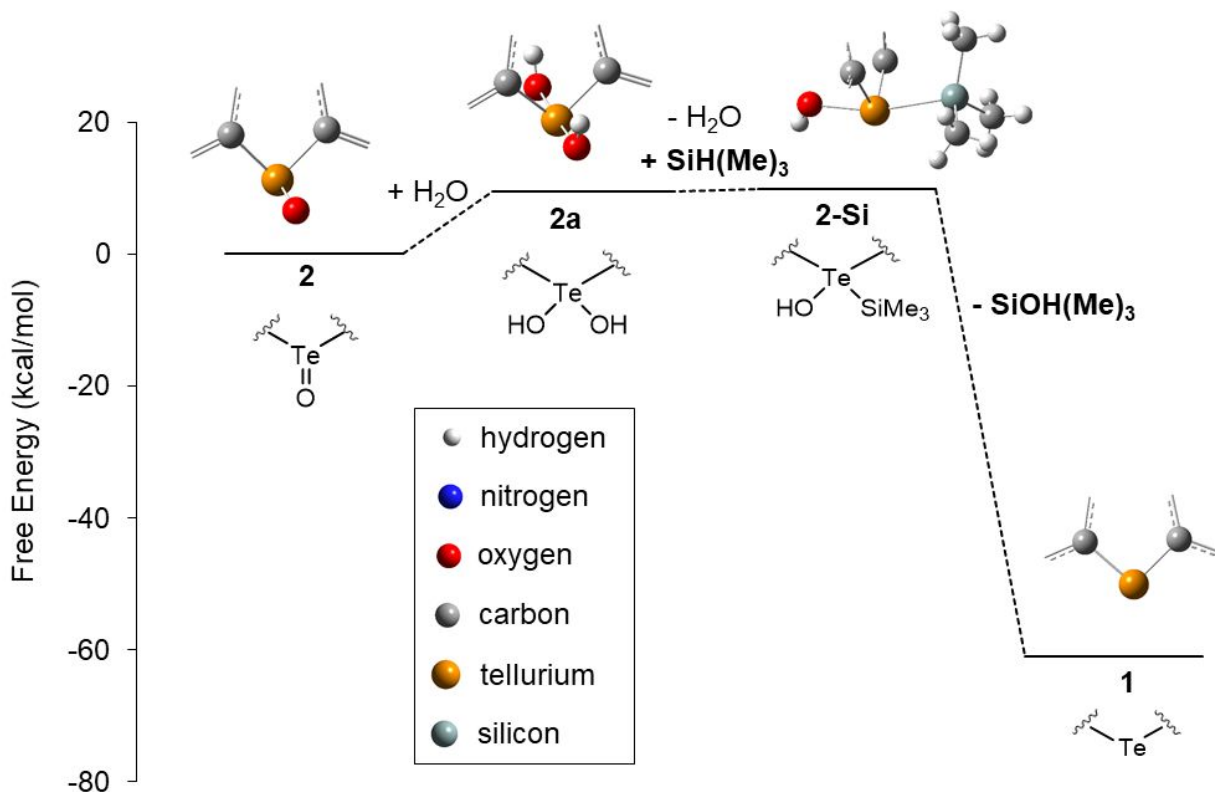


Figure 4. Reaction coordinate of trimethyl silane oxidation. Reductive elimination of silanol from the tellurium core of **2-Si** yields the reduced catalyst **1**.

4 Conclusion

Tellurorhodamine chromophores have a rich oxidation chemistry that has, until now, been relatively unexplored. We have successfully shown that both phosphine and various silanes can be catalytically oxidized by **1** to the corresponding phosphine oxide and silanols. Reaction kinetics of the oxidation of triphenyl phosphine and methyl diphenyl silane by **2** were explored. Substrate dependence on reaction kinetics was observed in both cases, which points to an associative substitution-like mechanism for both phosphine and silane.

The role of water in each oxidation reaction was explored. Kinetic isotope effect studies showed that hydrogen bonding from water solvent largely effects the relative rates of oxidation, with silane affected more so, likely due to explicit proton exchange with

water. Triphenyl phosphine and all silanes were catalytically oxidized within 18-24 hours with irradiation, confirmed by $^1\text{H}/^{13}\text{C}$ NMR spectroscopy and mass spectrometry.

The mechanisms by which **2** oxidizes phosphine and silane were also explored. Using the results of kinetic experiments and computation, different mechanisms were proposed for phosphine and silane oxidation. In the case of phosphine, direct addition to **2** affords a tetra-substituted intermediate before reductive elimination of phosphine oxide and regeneration of **1**. Substitution of phosphine on **2a** was found to be energetically unfavorable. Silane oxidation proceeded through a substitution-like mechanism wherein a single hydroxyl group from **2a** is displaced by silane, to form water and a silane bound intermediate **2-Si**. Similar reductive elimination from the tellurium core affords the corresponding silanol and **1**.

5 Conflicts of Interest

There are no conflicts to declare

6 Acknowledgments

This work was funded by the American National Science Foundation, Directorate for Mathematical and Physical Science, Division of Chemistry, award #1800599. Funding was also provided from the Portland State University Faculty Development Grant.

7 References

1. Anastas, P. T., Kirchoff, M. M. & Williamson, T. C. Catalysis as a foundational pillar of green chemistry. *Appl. Catal. A Gen.* **221**, 3–13 (2001).
2. Ritter, S. K. Green chemistry gets greener. *Chem. Eng. News* **80**, 38–42 (2002).
3. Campbell, A. N. & Stahl, S. S. Overcoming the ‘oxidant problem’: Strategies to use O₂ as the oxidant in organometallic C-H oxidation reactions catalyzed by Pd (and Cu). *Acc. Chem. Res.* **45**, 851–863 (2012).
4. Kawaoka, K., Khan, A. U. & Kearns, D. R. Role of singlet excited states of molecular oxygen in the quenching of organic triplet states. *J. Chem. Phys.* **46**, 1842–1853 (1967).
5. Demas, J. N., Harris, E. W. & McBride, R. P. Energy Transfer from Luminescent Transition Metal Complexes to Oxygen. *J. Am. Chem. Soc.* **99**, 3547–3551 (1977).
6. Tanielian, C., Wolff, C. & Esch, M. Singlet oxygen production in water: Aggregation and charge-transfer effects. *J. Phys. Chem.* **100**, 6555–6560 (1996).
7. Abdel-Shafi, A. A., Beer, P. D., Mortimer, R. J. & Wilkinson, F. Photosensitized generation of singlet oxygen from (substituted bipyridine)ruthenium(II) complexes. *Helv. Chim. Acta* **84**, 2784–2795 (2001).
8. Pefkianakis, E. K., Christodouleas, D., Giokas, D. L., Papadopoulos, K. & Vougioukalakis, G. C. A family of Ru(II) photosensitizers with high singlet oxygen quantum yield: Synthesis, characterization, and evaluation. *Eur. J. Inorg. Chem.* 4628–4635 (2013).
9. Abdel-Shafi, A. A., Ward, M. D. & Schmidt, R. Mechanism of quenching by

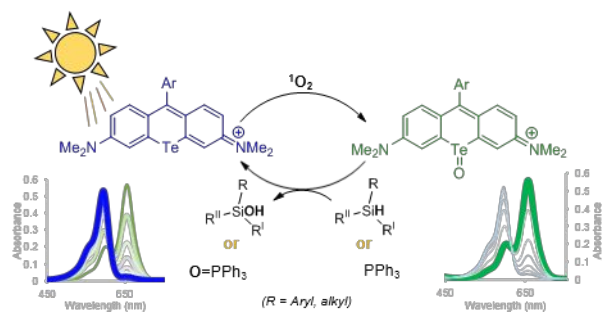
- oxygen of the excited states of ruthenium(ii) complexes in aqueous media. Solvent isotope effect and photosensitized generation of singlet oxygen, $O_2(^1\Delta_g)$, by $[Ru(\text{diimine})(CN)_4]^{2-}$ complex ions. *J. Chem. Soc. Dalton Trans.* 2517–2527 (2007).
10. Abdel-Shafi, A. A., Beer, P. D., Mortimer, R. J. & Wilkinson, F. Photosensitized Generation of Singlet Oxygen from Vinyl Linked Benzo-Crown-Ether-Bipyridyl Ruthenium(II) Complexes. *J. Phys. Chem. A* **104**, 192–202 (2000).
 11. Wang, F., Min, S., Han, Y. & Feng, L. Visible-light-induced photocatalytic degradation of methylene blue with polyaniline-sensitized TiO_2 composite photocatalysts. *Superlattices Microstruct.* **48**, 170–180 (2010).
 12. Oba, M., Endo, M., Nishiyama, K., Ouchi, A. & Ando, W. Photosensitized oxygenation of diaryl tellurides to telluroxides and their oxidizing properties. *Chem. Commun.* **2**, 1672–1673 (2004).
 13. Okada, Y., Oba, M., Arai, A., Tanaka, K., Nishiyama, K., Ando, W. Diorganotelluride-catalyzed oxidation of silanes to silanols under atmospheric oxygen. *Inorg. Chem.* **49**, 383–385 (2010).
 14. Oba, M., Tanaka, K., Nishiyama, K. & Ando, W. Aerobic oxidation of thiols to disulfides catalyzed by diaryl tellurides under photosensitized conditions. *J. Org. Chem.* **76**, 4173–4177 (2011).
 15. Oba, M., Okada, Y., Nishiyama, K. & Ando, W. Aerobic photooxidation of phosphite esters using diorganotelluride catalysts. *Org. Lett.* **11**, 1879–1881 (2009).
 16. Kryman, M. W.; Schamerhorn, G. A.; Hill, J. E.; Calitree, B. D.; Davies, K. S.;

- Linder, M. K.; Ohulchanskyy, T. Y.; Detty, M. R. Synthesis and Properties of Heavy Chalcogen Analogues of the Texas Reds and Related Rhodamines. *Organometallics* **33**, 2628–2640 (2014).
17. Detty, M. R. & Gibson, S. L. Tellurapyrylium Dyes as catalysts for the Conversion of Singlet Oxygen and Water to Hydrogen Peroxide. *J. Am. Chem. Soc.* **112**, 4086–4088 (1990).
 18. Calitree, B.; Donnelly, D. J.; Holt, J. J.; Gannon, M. K.; Nygren, C. L.; Sukumaran, D. K.; Autschbach, J.; Detty, M. R. Tellurium Analogues of Rosamine and Rhodamine Dyes: Synthesis, Structure, ¹²⁵Te NMR, and Heteroatom Contributions to Excitation Energies. *Organometallics* **26**, 6248–6257 (2007).
 19. Lutkus, L. V. Irving, H. E.; Davies, K. S.; Hill, J. E.; Lohman, J. E.; Eskew, M. W.; Detty, M. R.; McCormick, T. M. Photocatalytic Aerobic Thiol Oxidation with a Self-Sensitized Tellurorhodamine Chromophore. *Organometallics* **36**, 2588–2596 (2017).
 20. Mori, K., Tano, M., Mizugaki, T., Ebitani, K. & Kaneda, K. Efficient heterogeneous oxidation of organosilanes to silanols catalysed by a hydroxyapatite-bound Ru complex in the presence of water and molecular oxygen. *New J. Chem.* **26**, 1536–1538 (2002).
 21. Villemin, E.; Gravel, E.; Jawale, D. V.; Prakash, P.; Namboothiri, I. N. N.; Doris, E. Polydiacetylene Nanotubes in Heterogeneous Catalysis : Application to the Gold-Mediated Oxidation of Silanes. *Macromol. Chem. Phys.* **216**, 2398–2403 (2015).
 22. Jeon, M., Han, J. & Park, J. Transformation of Silanes into Silanols using Water and Recyclable Metal Nanoparticle Catalysts. *ChemCatChem* **4**, 521–524 (2012).

23. Minisci, F. Francesco. M.; Francesco, R.; Carlo, P.; Chiara, G; Francesca, F.; Gian Franco, P. A New, Highly Selective, Free-Radical Aerobic Oxidation of Silanes to Silanols Catalysed by N-Hydroxyphthalimide under Mild Conditions. *Synlett* **7**, 1173–1175 (2002).
24. Kryman, M. W.; Schamerhorn, G. A.; Yung, K.; Sathyamoorthy, B.; Sukumaran, D. K.; Ohulchanskyy, T. Y.; Benedict, J. B.; Detty, M. R. Organotellurium Fluorescence Probes for Redox Reactions: 9-Aryl-3,6-diaminotelluroxanthylum Dyes and Their Telluroxides. *Organometallics* **32**, 4321–4333 (2013).
25. Scalmani, G.; Frisch, M. J.; Mennucci, B.; Tomasi, J.; Cammi, R.; Barone, V. Geometries and properties of excited states in the gas phase and in solution: Theory and application of a time-dependent density functional theory polarizable continuum model. *J. Chem. Phys.* **124**, 094107 (2006).
26. Dennington, R., Keith, T. & Millam, J. GaussView, Version 5. *Semichem Inc.* , *Shawnee Mission, KS* Semichem Inc (2009). doi:10.1136/amiajnl-2013-001993
27. Becke, A. D. A new mixing of Hartree-Fock and local-density-functional theories. *J. Chem. Phys.* **98**, 1372–1377 (1993).
28. Miehlich, B., Savin, A., Stoll, H. & Preuss, H. Results obtained with the correlation energy density functionals of becke and Lee, Yang and Parr. *Chem. Phys. Lett.* **157**, 200–206 (1989).
29. Lee, C., Yang, W. & Parr, R. G. *Development of the Colle-Salvetti correlation-energy formula into a functional of the electron density. Physical Review B* **37**, 785–789 (1988).
30. Hehre, W. J., Ditchfield, R., Radom, L. & Pople, J. A. Molecular orbital theory of

- the electronic structure of organic compounds. V. Molecular theory of bond separation. *J. Am. Chem. Soc.* **92**, 4796–4801 (1970).
31. Ditchfield, R., Hehre, W. J. & Pople, J. A. Self-Consistent Molecular-Orbital Methods. IX. An Extended Gaussian-Type Basis for Molecular-Orbital Studies of Organic Molecules. *J. Chem. Phys.* **54**, 724–728 (1971).
 32. Hariharan, P. C. & Pople, J. A. The influence of polarization functions on molecular orbital hydrogenation energies. *Theor. Chim. Acta* **28**, 213–222 (1973).
 33. Hay, P. J. & Wadt, W. R. *Ab initio* effective core potentials for molecular calculations. Potentials for K to Au including the outermost core orbitals. *J. Chem. Phys.* **82**, 299–310 (1985).
 34. Hay, P. J. & Wadt, W. R. *Ab initio* effective core potentials for molecular calculations. Potentials for the transition metal atoms Sc to Hg. *J. Chem. Phys.* **82**, 270–283 (1985).
 35. Wadt, W. R. & Hay, P. J. *Ab initio* effective core potentials for molecular calculations. Potentials for main group elements Na to Bi. *J. Chem. Phys.* **82**, 284–298 (1985).
 36. Hirshfeld, F. L. Bonded-atom fragments for describing molecular charge densities. *Theor. Chim. Acta* **44**, 129–138 (1977).
 37. De Proft, F., Van Alsenoy, C., Peeters, A., Langenaeker, W. & Geerlings, P. Atomic charges, dipole moments, and Fukui functions using the Hirshfeld partitioning of the electron density. *J. Comput. Chem.* **23**, 1198–1209 (2002).

TOC



Silanes and phosphines are photocatalytically oxidized with a self-sensitized tellurorhodamine under aerobic conditions.